Effect of Carbon Dots on Supercapacitor Performance of Carbon Nanohorn/Conducting Polymer Composites

Chia Chi Chang, Tesfaye Abebe Geleta, and Toyoko Imae*

Conducting composites of carbon nanohorn (CNH), carbon dots and polyaniline or polypyrrole have been synthesized and evaluated the performance for supercapacitors. Results of specific capacitance and capacitance stability indicate that the addition of carbon dots to composites of CNH with conducting polymers provides the significant enhancing effect as promising electrode materials for energy storage devices.

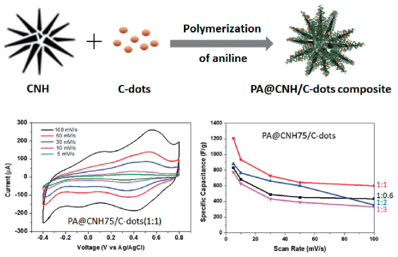

REPRINTED FROM

Bulletin of the Chemical Society of Japan

Vol.94 No.2 2021 p.454–462
February 15, 2021

The Chemical Society of Japan

BCSJ

Document type: Article

Effect of Carbon Dots on Supercapacitor Performance of Carbon Nanohorn/Conducting Polymer Composites

Chia Chi Chang,[1] **Tesfaye Abebe Geleta,**[1] **and Toyoko Imae***[1,2,3]

[1]Graduate Institute of Applied Science and Technology, National Taiwan University of Science and Technology, Taipei 10607, Taiwan

[2]Department of Chemical Engineering, National Taiwan University of Science and Technology, Taipei 10607, Taiwan

[3]Department of Materials Science and Engineering, National Taiwan University of Science and Technology, Taipei 10607, Taiwan

E-mail: imae@mail.ntust.edu.tw

Received: August 28, 2020; Accepted: October 26, 2020; Web Released: November 3, 2020

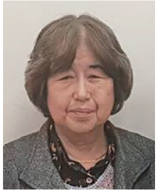

Toyoko Imae

Toyoko Imae received her Doctor of Science degree from Nagoya University. She joined the National Taiwan University of Science and Technology, Taiwan, as an honorary chair professor in April 2009, immediately after retiring from Keio University, Japan. She has also been professor emeritus of Nagoya University, Japan, since 2006. Her major research areas are the fabrication, functionalization, and physicochemical investigation of nanomaterials, including polymers, nanoparticles, carbon materials, minerals and their composites. Her present research target is “Nanoarchitecture and Nanotechnology” towards energy, environmental and biomedical sciences.

Abstract

Conducting composites consisting of carbon nanohorn (CNH), carbon dots (C-dots) and polyaniline (PA) or polypyrrole (PP) have been synthesized via in-situ polymerization and evaluated for performance as electrode materials for supercapacitors. The addition of C-dots to composites of CNH and conducting polymer showed a superior influence on supercapacitance properties in comparison with composites without C-dots. Incidentally, the specific capacitance was 1206 F/g and 538 F/g at a scan rate of 5 mV/s for composites of CNH with PA and PP, respectively, with addition of C-dots. These values were 1.6 and 2.3 times higher than values for composites without C-dots. Moreover, composites with C-dots exhibited high capacitance retention (94 and 93%, respectively). Thus, these results indicate that the addition of C-dots to composites of CNH with conducting polymers provides a significant enhancing effect as promising electrode materials for energy storage devices with high capacitance and stability.

Keywords: Carbon nanohorn/conducting polymer/carbon dot composite | Supercapacitor performance | Specific capacitance

1. Introduction

With the growing requirements for global renewable energy, the development of novel electrode materials of supercapacitors is an important issue in energy storage research, because the characteristics of supercapacitor devices are fundamentally determined by the structures and electrochemical properties of electrode materials.[1,2] Supercapacitors based on different charge storage mechanisms can be classified into two types; The charge can be stored by the electrostatic interaction at the electrode-electrolyte interface (the electrochemical double layer capacitor (EDLC) consisting of carbon material) or by the redox process (pseudocapacitor (PC) consisting of conducting polymer or metal oxide).[3–6] However, EDLCs and PCs have the inherent disadvantages of relatively low specific capacitance and poor cycle life, respectively. In order to alleviate these disadvantages, hybrid of EDLC material with PC material could be responsible for high specific capacitance, excellent chemical/thermal stabilities and long cycle life. Thus, it is called a hybrid supercapacitor.[7]

In the last several years, many different EDLC-PC hybrid electrode materials have been investigated to achieve enhanced capacitances and improve the charge-discharge rate capabilities, although some materials have been relatively high cost, inconvenient to synthesize and non-environmentally friendly.[8–10] Among conducting polymers, polyaniline (PA) and polypyrrole (PP) are commonly used as active PC materials due to their good electrical conductivity in doping state and easy availability.[11,12] Thus, PA or PP has been hybridized with EDLC materials like carbon nanotube (CNT), graphene, graphene oxide (GO) and reduced CNT for fabricating electrodes of supercapacitors to improve electrochemical performance.[5,13–15] However, only a few research groups have studied carbon nanohorn (CNH) or

© 2021 The Chemical Society of Japan

carbon quantum dots (C-dots), a new family of carbon materials, combined with PA or PP as an electrode.[16–19]

CNH is composed of nano-sized graphitic horns and takes a globular structure like a dahlia-flower with a diameter of 80–100 nm. It possesses internal nanospace, excellent electric conductivity and high purity, since no metal catalyst is involved in their synthesis.[20–23] On the other hand, C-dots are a new class of carbon materials with a size below 5 nm containing a conjugated structure[24] and exhibit numerous superior merits such as strong fluorescence, high water dispersibility, high chemical stability and simple surface functional groups (e.g., carboxyl and amine), making them emerge as an attractive material in various fields. Especially, C-dots as active components in electronic devices which can help to avoid the restacking of other components, improve porosity and ion diffusion, and enhance electron transfer within the electrode materials.[25–30] Thus, we have reported that a composite of CNH and PA at 75:25 wt% exerts synergetic effects as a hybrid supercapacitor,[19] and the hybridization of C-dots with PA and PP enhances capacitance.[18]

In this study, for composites of CNH (EDLC material) and conducting polymers (PC material), C-dots were added as third electrode material for hybrid supercapacitors, and the effect of C-dots was investigated for their electrochemical behaviours by cyclic voltammetry (CV), galvanostatic charge-discharge (GCD) and electrochemical impedance spectroscopy (EIS). Thus, the addition of C-dots on hybrid supercapacitors of CNH with conducting polymers is expected to bring superior electrochemical performance in comparison with hybrid supercapacitors composed of CNH/conductive polymers[19] or conductive polymers/C-dots.[18]

2. Experimental

Reagents and Materials. Pyrrole monomer (99%), aniline monomer (99.5%), citric acid (CA, anhydrous), ethylenediamine (EDA, 99+%) and ammonium persulfate (APS, 98+%) were purchased from Acros Organics (UK). Hexadecytrimethylammonium bromide (CTAB) and Nafion® (perfluorinated resin) solution (5 wt% in lower aliphatic alcohols and water, contains 15–20% water) were purchased from Sigma-Aldrich (USA). CNH was purchased from NEC (Japan). Indium tin oxide (ITO) glass was purchased from AimCore Technology (Taiwan). Other reagents were of analytical grade and all reagents were used as received. In all the experiments, distilled deionized water with resistivity 18.2 MΩ•cm was used.

C-dots with different nitrogen contents were synthesized according to previous reports.[28,29] Briefly, CA (1 g) was dissolved in water (10 ml) under sonication for 5 min and then added EDA (0.2, 0.3, 0.7 and 1 ml), for which the calculated mole ratio of CA to EDA was 1:0.6, 1:1, 1:2 and 1:3. The solution was heated at 230 °C for 5 h in a Teflon-coated autoclave and thus, a brown transparent C-dots dispersion was obtained. The synthesis scheme is illustrated in Figure 1a.

Synthesis of Polymer@CNH Composites with C-Dots. The composites of CNH with conducting polymers and C-dots were synthesized according to the following procedure:[9] The CNH was dispersed with CTAB (124 mg) in an aqueous 1 M HCl solution (31 ml) under sonication for 30 min. Then to the dispersion was added the C-dots dispersion (0.5 ml) at different nitrogen contents and sonicated for 30 min at room temperature (~25 °C). The mixed dispersion, to which was added aniline monomer (60 µl) or pyrrole monomer (60 µl), was added dropwise a freshly prepared an aqueous 0.14 M APS solution. The in-situ polymerization process was carried out in an ice bath for 24 h. After filtration, the resulting composites were subsequently washed with ethanol and water until being neutralized, and the products were dried at 50 °C overnight. Then the weight ratio of polymer and CNH was 25:75, and thus the composites were named polymer@CNH75/C-dots(1:x), x = 0.6, 1, 2, and 3. The composites of polymer/C-dots(1:x) were also synthesized by way of comparison. Then the content of C-dots in polymer@CNH75/C-dots and polymer/C-dots was 9.5 wt%. The synthesis process of composites is illustrated in Figure 1b.

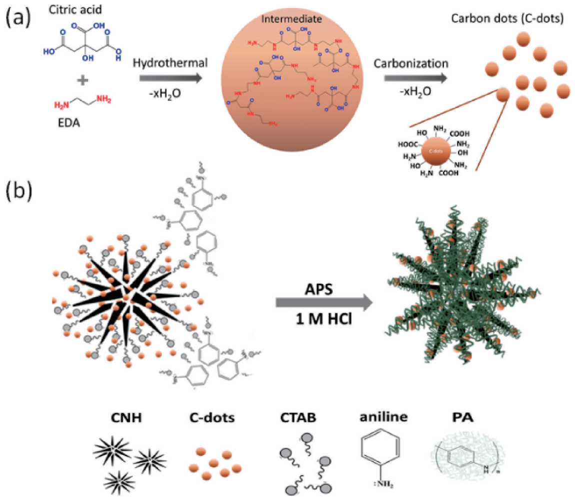

Figure 1. A schematic illustration of synthesis processes of (a) C-dots and (b) PA@CNH/C-dots composites.

Instruments. Field emission scanning electron microscopic (FE-SEM) observation was performed on a JEOL JSM-6500F microscope (Japan). Fourier transform infrared (FTIR) absorption spectra were recorded in KBr pellets using a Nicolet thermo scientific 6700 (USA). Thermogravimetric analysis (TGA) was done using a TA Q500 appliance (USA) from 25 °C to 1000 °C at a heating rate of 10 °C/min under nitrogen flow. Nitrogen physical adsorption was performed with a BELSORP-max instrument (Japan) using N_2 gas as an adsorbate. Before the adsorption measurements, the powders were degassed at 130 °C for 2 h. The specific surface area was calculated based on the Brunauer-Emmett-Teller (BET) analysis from the N_2 adsorption isotherms. The pore size distribution was obtained from the desorption isotherms on the Barrette-Joyner-Halenda (BJH) basis.

Electrochemical measurements were carried out using a Zahner Zennium electrochemical workstation (Germany) with a conventional three-electrode system of a working electrode, an Ag/AgCl reference electrode and a Pt wire counter electrode in a 1 M NaCl electrolyte solution. ITO glass as a working electrode was cleaned with a detergent solution, acetone, ethanol, and water, and then treated with ultraviolet light (172 nm) to remove a variety of organic contaminants from the surface.

Subsequently, the electrode compound (15 mg) was dispersed in ethanol (1 ml) and then Nafion (250 µl) was added to form a slurry. The slurry was then spin-coated on ITO glass with a 1 cm^2 geometric area and dried at 50 °C. The CV and GCD measurements were performed in an aqueous 1 M NaCl electrolyte solution at controlled potential window (−0.4 to 0.8 V) and current density (1 to 10 A/g). EIS measurement was carried out in the frequency range of 100 mHz to 100 kHz at the open circuit potential of 5 mV amplitude.

The gravimetric specific capacitance, C_s [Fg^{-1}], was calculated from CV curves according to eq (1) as follows:

$$C_s = \int \frac{I}{m}\frac{dV}{v\Delta V}, \tag{1}$$

where I [A] is the current, m [g] is the mass of active material, V [V] is the potential, v [V/s] is the scan rate, and ΔV [V] is the potential window.[5,19,31]

3. Results and Discussion

Characterization of Composites. While CNH exhibited a dahlia-like shape with diameter ranging from 80 to 100 nm and PA and PP showed irregular shape and nanowire shape, respectively, the hybrids of CNH with PA and PP took a shape like pristine CNH, as reported previously.[19] A similar situation arose with the addition of C-dots, as seen in Figure 2, although C-dots could not be distinguished in TEM and SEM images, because of their small size (<5 nm),[15] a small amount (9.5 wt%) against polymer@CNH and the same X-ray density as CNH.

Chemical structures of conducting polymer@CNH75/C-dots(1:1) composites were identified by FTIR absorption spectroscopy and compared to polymer@CNH75 without C-dots (Figure 3). The IR spectrum of PA@CNH75/C-dots(1:1) showed strong IR bands at 1570 and 1125 cm^{-1}, which correspond to IR bands (1561 and 1179 cm^{-1}) of CNH attributed to CC stretching vibration mode.[19] The relevant bands for PP@CNH75/C-dots(1:1) were observed at 1548 and 1177 cm^{-1}. The additional characteristic IR bands (1518 and 1291 cm^{-1}) of PA@CNH75/C-dots(1:1) originated in PA.[19] However, IR absorption spectra of polymer@CNH75/C-dots(1:1) were similar to those of polymer@CNH75 but did not distinctly display characteristic IR bands (1693 and 1398 cm^{-1}) of C-dots due to a smaller quantity of C-dots in comparison with the amount of polymer@CNH in composites.

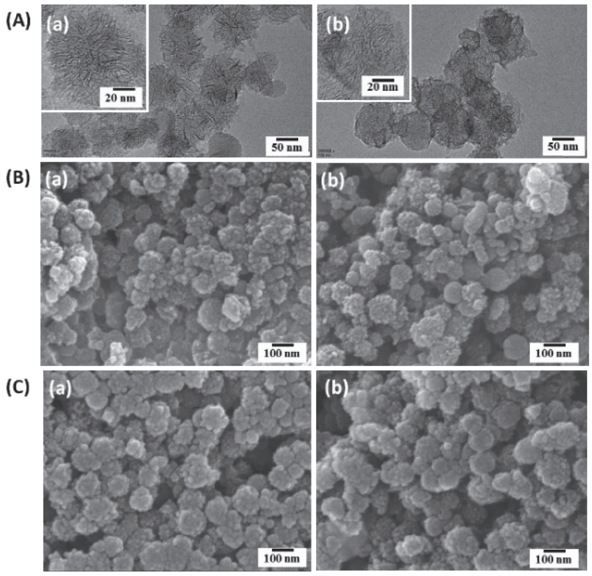

Figure 2. (A) TEM and (B), (C) FE-SEM images of (a) PA@CNH75/C-dots(1:1) and (b) PP@CNH75/C-dots(1:1). (B) Before and (C) after 2000 cycles charge/discharge measurement.

The XRD pattern of C-dots (Figure 4) exhibited a broad peak at 1°, which clearly indicates the (002) plane of small size of C-dots.[32,33] After hybridizing with CNH and conducting

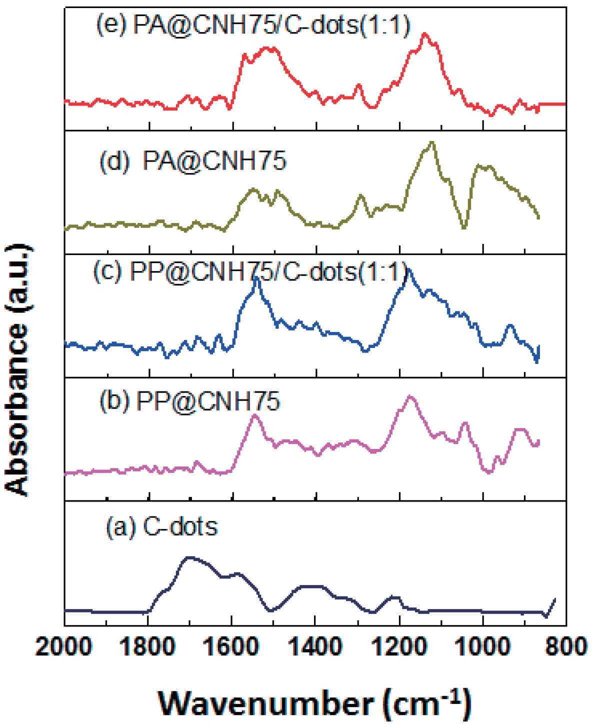

Figure 3. FT-IR spectra of (a) C-dots, (b) PP@CNH75, (c) PP@CNH75/C-dots(1:1), (d) PA@CNH75 and (e) PA@CNH75/C-dots(1:1).

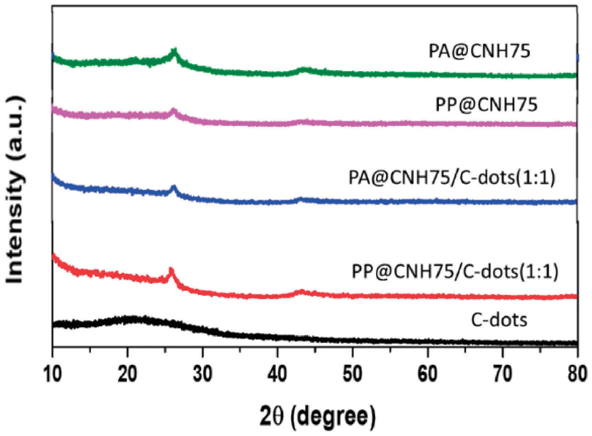

Figure 4. XRD patterns of C-dots, PA@CNH75, PA@CNH75/C-dots(1:1), PP@CNH75 and PP@CNH75/C-dots(1:1).

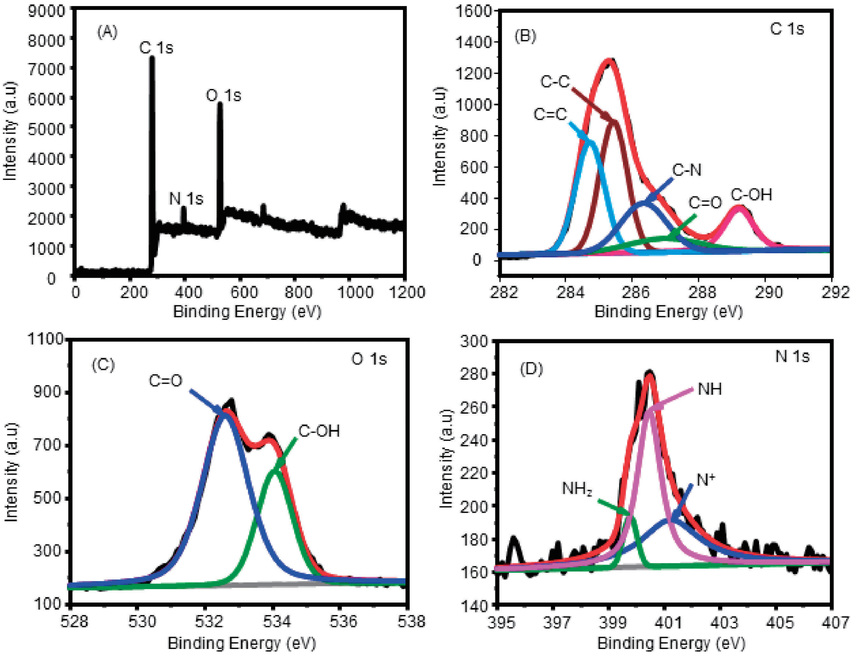

Figure 5. (A) XPS full survey spectra of PP@CNH75/C-dots(1:1) and the deconvoluted spectra of (B) C 1s, (C) O 1s and (D) N 1s.

Table 1. Binding energy and area intensity obtained from XPS of PP@CNH75/C-dots(1:1) nanocomposite.*

Element	PP@CNH75/C-dots(1:1)		Assignment
	Binding energy (eV)	Area intensity (a.u.)	
C 1s	284.7	791.2	C=C^{a,b,c} (aromatic)
	285.4	889.9	C-C^{a,b,c} (aromatic(sp^2)/aliphatic(sp^3))
	286.3	546.5	C-N^{b,c} (pyrrolic/amine)
	286.7	257.2	C=O^{c} (carboxylic)
	289.2	363.4	C-OH^{c} (carboxylic)
N 1s	399.8	19.1	$NH_2{}^{c}$ (amine)
	400.5	136.9	NH^{b} (pyrrolic)
	401.2	111.0	N$^{+\,b}$ (deprotonated pyrrolic)
O 1s	532.6	1352.2	C=O^{c} (carboxylic)
	534.1	616.3	C-OH^{c} (carboxylic)

*a = carbon nanohorn (CNH), b = polypyrrole (PP) and c = carbon dots (C-dots(1:1)).

polymer, sharper peaks appeared at 26° and 43°. These peaks can be assigned to (002) and (100) crystalline CNH,[19,34] because similar XRD bands were observed even for polymer@CNH75 without C-dots. XRD results also did not prove the existence of C-dots in the composites.

The chemical composition and species in the composites were characterized by XPS. The full XPS survey scan of PP@CNH75/C-dots(1:1) in Figure 5A exhibited the characteristic peaks of C 1s, N 1s, and O 1s. The binding energy values and area intensities of deconvoluted species obtained from the fine analysis in Figure 5(B-D) are listed in Table 1. On a C 1s peak, PP@CNH75/C-dots(1:1) possessed four deconvoluted species, which can be attributed to C=C (284.7 eV), aromatic (sp^2)/aliphatic (sp^3) C-C (285.4 eV), pyrrolic/amine C-N (286.3 eV), carboxylic C=O (286.7 eV) and phenolic C-OH (289.2 eV) bonds originating from CNH,[35] PP,[36] and C-dots.[37] The O 1s peak was deconvoluted into two species located at 532.6 and 534.1 eV occurring from carboxylic C=O and C-OH bonds of C-dots(1:1), respectively. Moreover, the N 1s peak revealed the major peak component at a binding energy of 400.5 eV assigned to pyrrolic -NH-, the high binding energy shoulder at 401.2 eV contributed from the deprotonated pyrrole -N$^+$- and the low binding energy component at 399.8 eV originating from amine (C-NH_2) bond in C-dots.[37] Thus, the coexistence of components of CNH, PP and C-dots in the composite was successfully confirmed from XPS spectra.

The weight loss on TGA during the temperature increase to 1000 °C was compared to confirm the thermal stability of polymer@CNH/C-dots composites and to estimate the interaction of C-dots with polymer@CNH. Because the measurement was performed under a nitrogen atmosphere, we can see only the thermal decomposition. As shown in Figure 6, the entrapped water molecules are removed at the first weight drop up to 100 °C. The thermal decomposition of C-dots will happen for carboxyl and amine moieties but less for graphitic cores and the remaining weight was only about 30% at 1000 °C. The thermal decomposition of PA@CNH and PP@CNH are less and the remaining was about 70 wt% at 1000 °C. When these decompositions were compared with polymer@CNH/C-dots, the decomposition of PA@CNH/C-dots were nearly similar to that

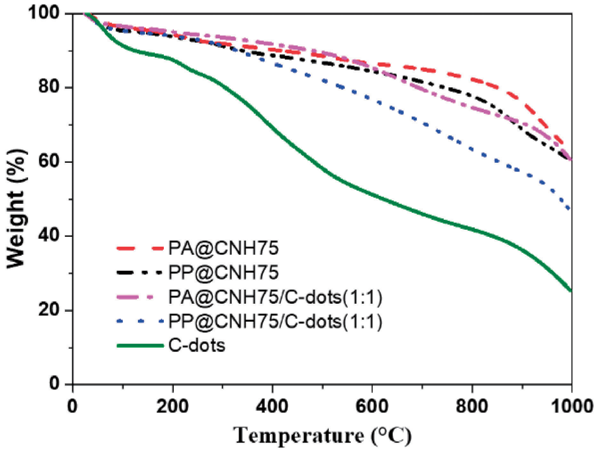

Figure 6. TGA curves of C-dots, PA@CNH75, PA@CNH75/C-dots(1:1), PP@CNH75 and PP@CNH75/C-dots(1:1).

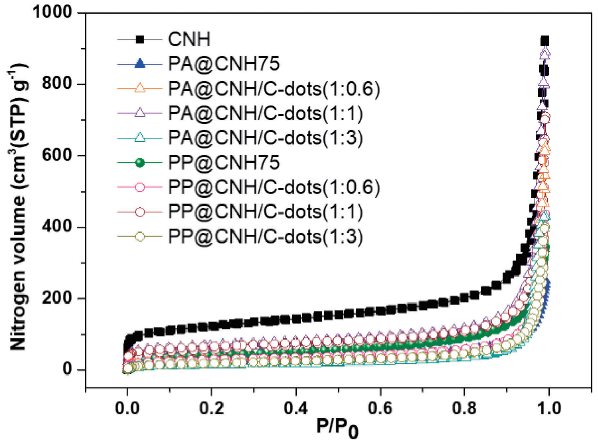

Figure 7. Nitrogen adsorption-desorption isotherms of CNH, polymer@CNH75, polymer@CNH75/C-dots(1:x, x = 0.6, 1 and 3).

of PA@CNH but the decomposition of PP@CNH/C-dots was larger than that of PP@CNH. These results indicate that PA@CNH/C-dots composite is thermally more stable than PP@CNH/C-dots and the interaction of C-dots was stronger with PA@CNH than with PP@CNH. An estimated difference of the interaction of C-dots to polymers will be valuable to explain the difference on polymer@CNH/C-dots capacitance.

The BET analyses were carried out to determine the surface area and pore-size distribution of the conducting polymer@CNH/C-dots composites from nitrogen physical adsorption-desorption isotherms at 77 K as shown in Figure 7. These isotherm profiles can be categorized as type II according to the IUPAC classification. Distinct differences in the adsorption were observed between CNH and polymer@CNH75 and polymer@CNH75/C-dots(1:x, x = 0.6, 1 and 3). CNH had a steep uptake at a low relative pressure (P/P_0), suggesting interstitial pores which formed between the adjacent CNHs.[38,39] However, the uptake sorption below $P/P_0 = 0.03$ in the isotherm curves of the composites became less with loading of C-dots on conducting polymers. Incidentally, the pore size distribution of composites displayed very weak intensities and no distinct pore peaks. The numerical values of surface area of the composites are listed in Table 2. The variation of CA:EDA mole ratio in C-dots on polymers@CNH75 first increased the surface area and then decreased it. Apparently, C-dots(1:1) was an optimized amount for this character of polymers@CNH75, and the effect of C-dots was nearly similar to both PA@CNH75 and PP@CNH75.

Electrochemical Performance. The electrochemical properties of the composites were examined by CV measurements with a three-electrode system in an aqueous 1 M NaCl solution as an electrolyte. Figure 8 shows CV curves of PA@CNH75/C-dots-series composites at different CA:EDA mole ratios at various scan rates. In comparison with conducting polymers@CNH75 without C-dots,[19] the CV curves of PA@CNH75/C-dots-series composites displayed clear redox

Table 2. Surface area, pore volume, specific capacitance, capacitance retention and charge transfer resistance of conducting polymer@CNH75/C-dots(1:x, x = 0.6, 1, 2, 3) at different C-dots(1:1) contents (0.2, 0.5, and 1.0 ml) and C-dots.

	PA@CNH7/ C-dots(1:0.6)	PA@CNH75/ C-dots(1:1)			PA@CNH7/ C-dots(1:2)	PA@CNH75/ C-dots(1:3)	C-dots
		0.2 ml	0.5 ml	1.0 ml			
Specific surface area (m^2g^{-1})	85.4	—	215.9	—	—	52.3	—
Specific capacitance (F/g) at 5 mV/s	829	193	1206	1127	881	772	12
Charge transfer resistance (Ω)	—	—	1.04	—	—	—	14.84
Capacitance retention (%)	—	—	97.3	—	—	—	—
	PP@CNH7/ C-dots(1:0.6)	PP@CNH75/ C-dots(1:1)			PP@CNH7/ C-dots(1:2)	PP@CNH75/ C-dots(1:3)	
		0.2 ml	0.5 ml	1.0 ml			
Specific surface area (m^2g^{-1})	95.1	—	202.1	—	—	70.7	
Specific capacitance (F/g) at 5 mV/s	183	304	642	251	549	215	
Charge transfer resistance (Ω)	—	—	4.62	—	—	—	
Capacitance retention (%)	—	—	94.6	—	—	—	
	PP/ C-dots(1:0.6)		PP/ C-dots(1:1)		PP/ C-dots(1:2)	PP/ C-dots(1:3)	
Specific capacitance (F/g) at 5 mV/s	182		922		420	153	

© 2021 The Chemical Society of Japan

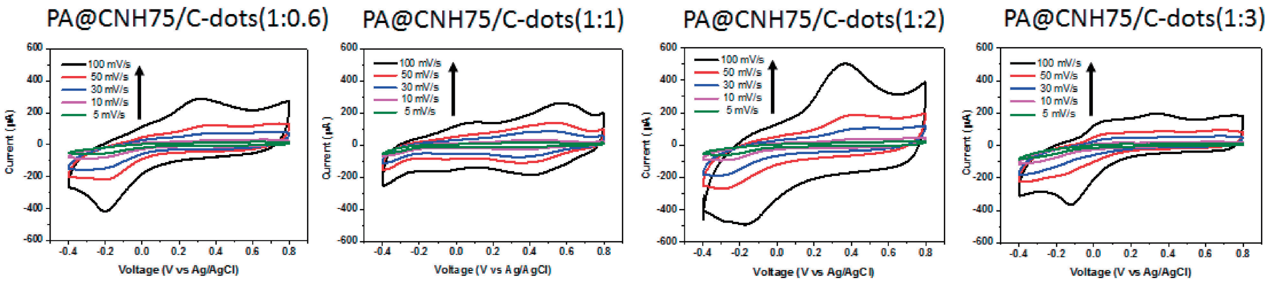

Figure 8. CV curves of PA@CNH75/C-dots(1:x, x = 0.6, 1, 2 and 3).

peaks besides EDLC shape, meaning the ideal capacitance behaviour,[40] although the redox properties were not remarkable for PP@CNH75/C-dots-series.

The specific capacitance values of the electrodes could be calculated based on eq (1) and the values at 5 mV/s scan rate are listed in Table 2, where values observed with PP@CNH75/C-dots-series and PP@C-dots-series composite electrodes are also included. The values are plotted in Figure 9 as a function of scan rate. The specific capacitance of PA@CNH75/C-dots-series electrodes increased at higher EDA ratio (C-dots(1:1)) than at lower ratio (C-dots(1:0.6)) but deceased with increasing further higher ratios (C-dots(1:2) and C-dots(1:3)). Moreover, the decrease of the specific capacitance with increasing scan rate was liberally different from polymer@C-dots without CNH.[18] These tendencies were obtained even for electrodes of PP@CNH75/C-dots-series and PP@C-dots-series without CNH. The highest specific capacitance (1206 F/g) at a scan rate of 5 mV/s was obtained for PA@CNH75/C-dots(1:1), and it was higher than that of PP@CNH75/C-dots(1:1) (642 F/g), and PP@C-dots(1:1) (922 F/g) and C-dots (12 F/g) (see Table 2), although these values were higher than the corresponding PA@CNH75 (762 F/g), PP@CNH75 (231 F/g) and PP (769 F/g) without C-dots.[19]

In addition, we have further studied the effect of C-dots content on the electrochemical properties of conducting polymers@CNH75/C-dots(1:1) electrodes. As seen in Table 1, the specific capacitance of conducting polymers@CNH75/C-dots(1:1) with different C-dots contents (0.2, 0.5 and 1 ml), where the content of C-dots in polymers@CNH75/C-dots was 4, 9.5 and 17.4 wt%, displayed that C-dots content at 0.5 ml had the highest specific capacitance. The adsorption of C-dots on the surface of conducting polymers@CNH75 accelerates the charge transfer, but the coating by excessive amount of C-dots would decrease the electrical conductivity. The specific capacitance of C-dots electrode is only 12 F/g at 5 mV/s, as listed in Table 2. Thus, the existence of a large amount of C-dots destroys the conductive channel consisting of CNH and polymer and depresses the capacitance.

The capacitive performance of electrodes was further investigated by GCD. The almost symmetric linear geometry of GCD curves as seen in Figure 10 indicates that conducting polymer@CNH75/C-dots(1:1) composites as the electrodes in supercapacitor exhibit high reversibility and ideal capacitive behavior.[41] Moreover, the PA@CNH75/C-dots(1:1) electrode possessed a longer discharge time than other electrodes, implying that such an electrode has an enhanced capacitance. These tendencies are alike as those from CV.

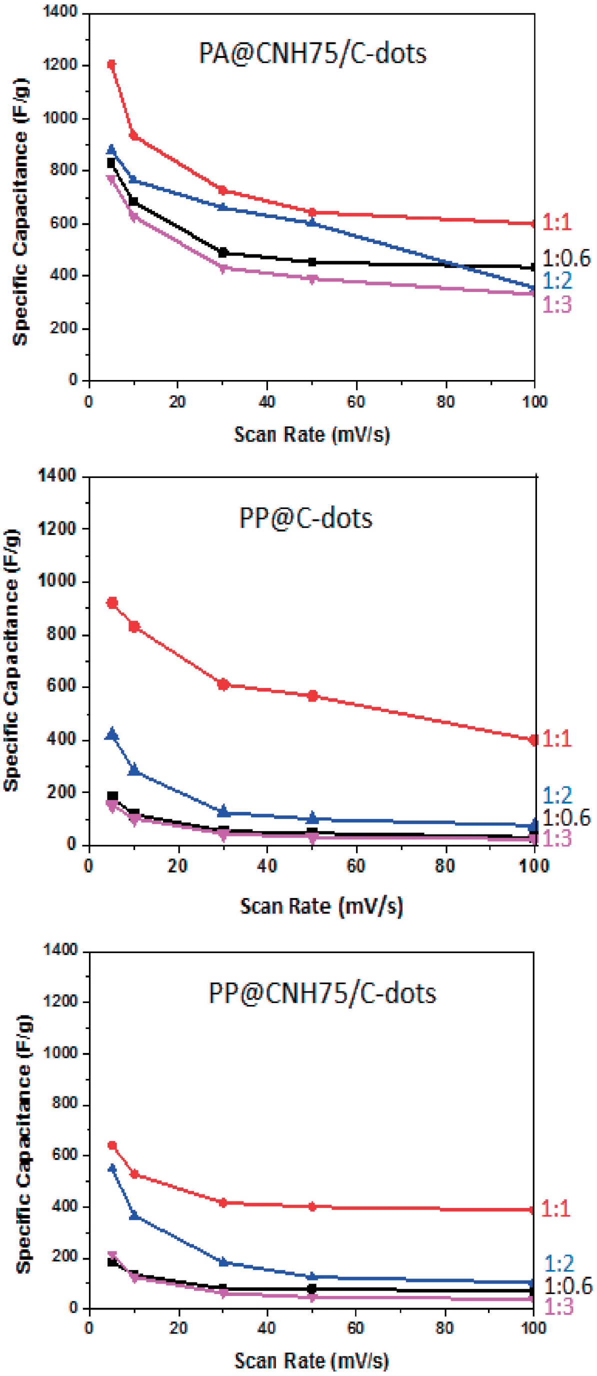

Figure 9. Specific capacitance as a function of scan rate of PA@CNH75/C-dots(1:x), PP/C-dots(1:x) and PA@CNH75/C-dots(1:x) at x = 0.6, 1, 2 and 3.

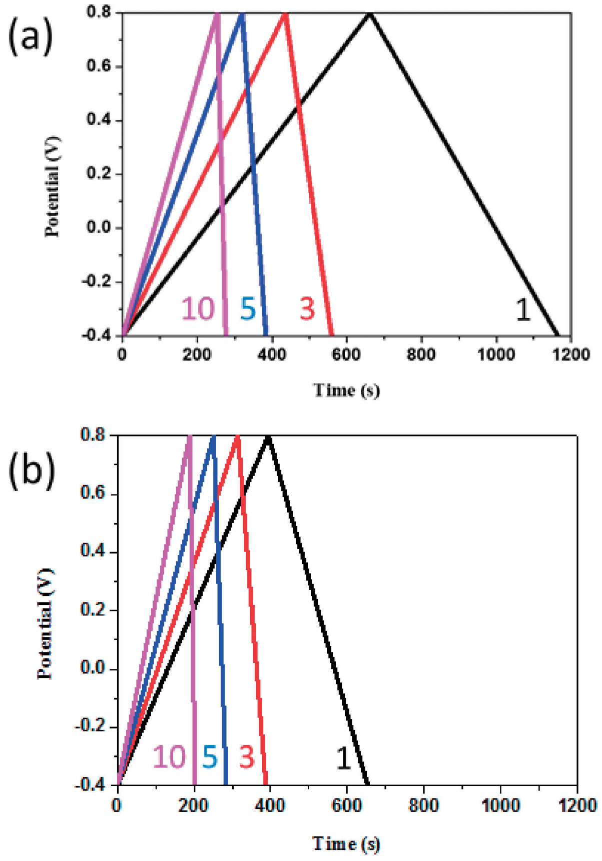

Figure 10. Charge/discharge curves of (a) PA@CNH75/C-dots(1:1) and (b) PP@CNH75/C-dots(1:1) electrodes at current densities of 1, 3, 5 and 10 A/g.

Furthermore, the cycling stability of both PA@CNH75/C-dots(1:1) and PP@CNH75/C-dots(1:1) were tested by GCD at a current density of 50 A/g. The capacitance of both electrodes retained 94 and 93% on average, respectively, of their initial capacitance even after 4000 cycles (Figure 11A and B). The simultaneously calculated averaged Coulombic efficiency (Figure 11C) was 102 and 103%, respectively. The FE-SEM images of before and after cycling stability are presented in Figure 2C. It was found that the morphologies of electrode materials seem nearly maintained, indicating the good reversibility for both electrodes.

The enhanced electrochemical properties for conducting polymers@CNH75 with different CA:EDA mole ratios of C-dots composites, especially, PA@CNH75/C-dots(1:1) in this work can be attributed to several reasons. Firstly, the homogenous and highly porous structure of the conducting polymers@CNH75/C-dots(1:1) facilitates the transfer of ions to contact with them, having more redox reactions. As shown in Table 2, the surface area and the internal pore volume were highest at the 1:1 content of C-dots in conducting polymers@CNH75/C-dots, where the accessibility of many electrolytes by the adsorption on the electrode surface may be responsible for increasing the specific capacitance.

Secondly, the electric resistance may be reduced by C-dots. Nyquist plots of PA@CNH75/C-dots(1:1) and PP@CNH75/C-dots(1:1) electrodes were shown in Figure 11D with their fitted equivalent circuit,[42] and the fitting results were compared

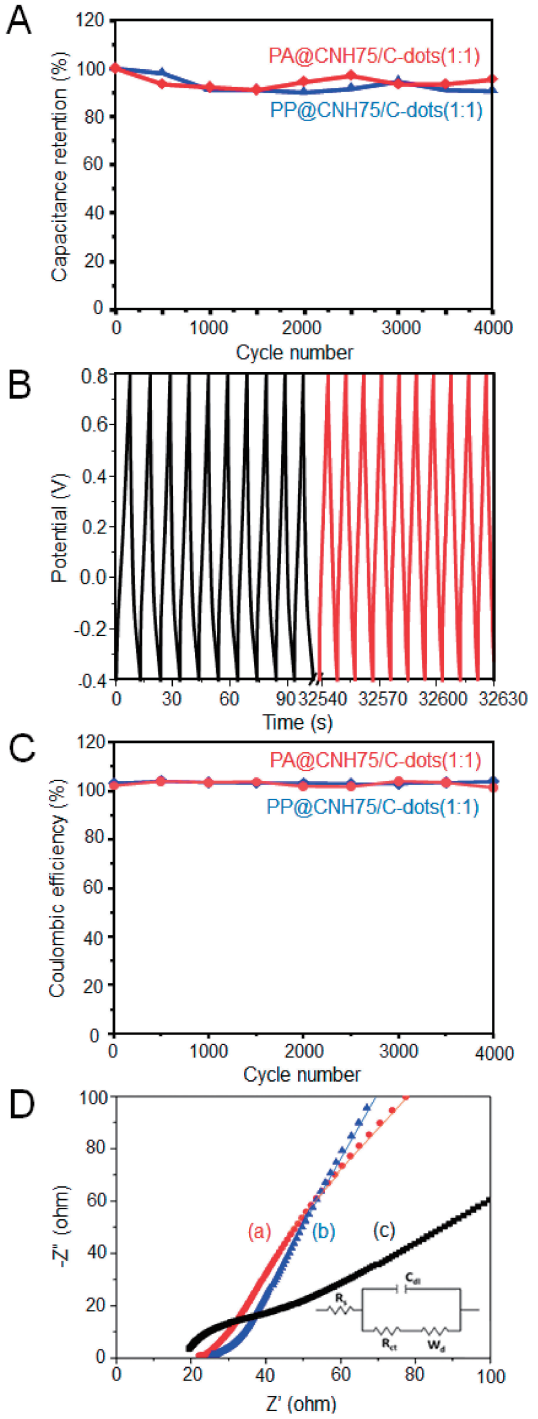

Figure 11. (A) Capacitance retention as a function of cycle number for PA@CNH75/C-dots(1:1) and PP@CNH75/C-dots(1:1) electrodes, (B) charge/discharge curves of the first 10 cycles and the last 10 cycles for PA@CNH/C-dots(1:1) composite electrode, (C) Coulombic effect as a function of cycle number for PA@CNH75/C-dots(1:1) and PP@CNH75/C-dots(1:1) electrodes, and (D) Nyquist plots of (a) PA@CNH75/C-dots(1:1), (b) PP@CNH75/C-dots(1:1) and (c) C-dots electrodes at frequencies ranging from 100 mHz to 100 kHz. Inset shows the electrical equivalent circuit, where R_s, R_{ct}, C_{dl}, and W_d are an ohmic series resistance, a charge transfer resistance, an EDLC and a Warburg diffusion impedance, respectively.

© 2021 The Chemical Society of Japan

Table 3. Recently published data of carbon-based electrode materials for supercapacitors in comparison with the present results of polymer@CNH75/C-dots.

Electrode material	Electrolyte	Scan rate (mV/s)/ current density (A/g)	Specific capacitance (F/g)	Ref.
CNH/single-walled carbon nanotube	1 M Et4NBF4/propylene carbonate	0.1 A/g	46	21
PA/CNH	1 M H_2SO_4	50 mV/s	168	45
PA/CNH	1 M KCl	5 mV/s	834	44
PP/Sulfonated Graphene	1 M H_2SO_4	1 A/g	360	48
PA/magnetic graphene	1 M NaCl	5 mV/s	253	5
PA/multiwalled carbon nanotube	1 M H_2SO_4	4.0 A/g	240	49
Graphene/PP/carbon nanotube	1 M KCl	0.2 A/g	361	46
PP/C-dots	1 M KCl	0.5 A/g	306	47
PP/C-dots	1 M NaCl	5 mV/s	754	18
		1 A/g	676	
PA/C-dots	1 M NaCl	5 mV/s	569	18
		1 A/g	529	
PP/graphene oxide/C-dots	1 M KCl, HCl, H_2SO_4, LiCl	0.5 A/g	508–582	17
Nitrogen-doped graphene	1 M NaCl	5 mV/s	303	15
Nitrogen-doped CNH	1 M NaCl	5 mV/s	248	15
PA@CNH	1 M NaCl	5 mV/s	762	19
PP@CNH	1 M NaCl	5 mV/s	231	19
PA@CNH/C-dots	1 M NaCl	5 mV/s	1206	Our work
PP@CNH/C-dots	1 M NaCl	5 mV/s	538	Our work
PP/C-dots	1 M NaCl	5 mV/s	922	Our work

with that of C-dots and listed in Table 2. The charge transfer resistance (1.04 Ω) of PA@CNH75/C-dots(1:1) electrode was smaller than those (4.62 and 12 Ω) of PP@CNH75/C-dots(1:1) and C-dots, respectively, and this result is comparable to the higher specific capacitance of PA@CNH75/C-dots(1:1) than PP@CNH/C-dots series. It is also noted that the Nyquist plot line of PA@CNH75/C-dots(1:1) was more vertical than that of PP@CNH75/C-dots(1:1) at a low-frequency region, indicating a nearly ideal capacitive behaviour.[31,43]

Consequently, all the above-mentioned results demonstrate that the additional C-dots improved the capacitance properties of polymer@CNH. This behaviour is relative to the fact that the C-dots-added polymer@CNH maintains high specific surface areas and low charge-transfer resistance. The capacitance of the EDLC electrode increases with increasing the specific surface area.[19] Meanwhile, the relationship of the charge-transfer resistance to the capacitance is obvious, because the low charge-transfer resistance indicates the fast charge transfer at the electrode/electrolyte interface and results in the high capacitance. The electrochemical property of PA@CNH/C-dots(1:1) is better than PP@CNH/C-dots(1:1), because the incorporation of C-dots is stronger in PA@CNH75 than in PP@CNH75 as clarified by TGA. Additionally, the adsorption degree of C-dots on PA is usually higher than on PP. In other words, C-dots located between CNH and PA may provide an interconnected pathway between them and thus accelerate the charge transfer rate. As C-dots, CNH and PA with six-membered rings can be easily mutual-layered each other, C-dots may be attracted by the strong π-π stacking interaction force on PA@CNH75 composite, which can reduce the charge transfer resistance, enhance the electron transport, and thus improve the electrochemical performance.

Table 3 lists the published data of carbon-based electrode materials for supercapacitors. Maiti et al.[44] have synthesized fibre-like PA/CNH composites and obtained the specific capacitance of 834 F/g at 5 mV/s, which was as high as the value from PA@CNH75 electrode[19] but smaller than that from PA@CNH75/C-dots(1:1) electrode in the present work. Moreover, the cyclic stability of their electrode was low (84% at 500 cycles), indicating insufficient improvement of the disadvantage of the pseudocapacitor by conducting polymers in their composites. The specific capacitance can be improved by the incorporation of C-dots into the conductive materials. Jian et al.[47] have fabricated a PP/C-dots composite and its capacitance was 306 F/g at 0.5 A/g. The specific capacitance of their composite was smaller than PP/C-dots composites (922 F/g at 5 mV/s) in the present work. The specific capacitance of the graphene oxide/C-dots/PP electrode by Zhang et al.[17] was 508–582 F/g at 0.5 A/g, depending on electrolytes, and similar to it (538 F/g at 5 mV/g) of PP@CNH75/C-dots electrode in the present work, although both values were obtained at different measurement methods of constant current density or scan rate. Generally, because the capacitance is influenced by the composite components and electrolytes besides measurement conditions described above, such difference must be considered on the comparison. PA@CNH75/C-dots(1:1) is more effective in improving the specific capacitance. As defined in eq (1), the specific capacitance is dominated by current, which is evaluated by the flow of charges. PA@CNH composite constructs ready channels for the flow of charges but the embedded C-dots play a role to connect unchanneled sites in PA@CNH to generate an additional channel for the flow of charges because of the strong interactions of C-dots with CNH and PA. Such interconnection promotes the fast transfer of charges and increases the current in the electrode. By the way, PP/C-dots electrode without CNH was more effective than PP@CNH75/C-dots on supercapacitor as seen in Table 2 and 3.

4. Conclusions

C-dots on composites of CNH with conducting polymers were in-situ deposited. The electrochemical tests demonstrated that PA@CNH/C-dots and pp@CNH/C-dots electrodes provided 1.6 and 2.3 fold, respectively, higher specific capacitance than the values for composites without C-dots and excellent cycling stability after 4000 cycles. The effective incorporation of C-dots into composites of CNH with polymers could accelerate the charge transfer in the composite, leading to superior electrochemical performance. Such performance provides a promising approach to design and manufacture novel hybrid EDLC-PC electrode materials for future energy-related devices.

This investigation was partly supported by the Ministry of Science and Technology, Taiwan (MOST 107-2221-E-011-067-). CCC greatly acknowledges and appreciates National Taiwan University of Science and Technology, Taiwan, for financial support and the opportunity of a postdoctoral fellowship.

References

1 C. Liu, F. Li, L. P. Ma, H. M. Cheng, *Adv. Mater.* **2010**, *22*, E28.

2 Y. Zhai, Y. Dou, D. Zhao, P. F. Fulvio, R. T. Mayes, S. Dai, *Adv. Mater.* **2011**, *23*, 4828.

3 E. Frackowiak, F. Beguin, *Carbon* **2001**, *39*, 937.

4 C. Peng, S. Zhang, D. Jewell, G. Z. Chen, *Prog. Nat. Sci.* **2008**, *18*, 777.

5 M. M. M. Ahmed, T. Imae, *Phys. Chem. Chem. Phys.* **2016**, *18*, 10400.

6 M. M. M. Ahmed, T. Imae, Chapter 10 in Nanolayer Research, ed. T. Imae, Elsevier, Amsterdam, **2017**, pp. 353. doi:10.1016/B978-0-444-63739-0.00010-4.

7 A. Muzaffar, M. B. Ahmed, K. Deshmukh, J. Thirumalai, *Renewable Sustainable Energy Rev.* **2019**, *101*, 123.

8 C. Sengottaiyan, R. Jayavel, R. G. Shrestha, T. Subramani, S. Maji, J. H. Kim, J. P. Hill, K. Ariga, L. K. Shrestha, *Bull. Chem. Soc. Jpn.* **2019**, *92*, 521.

9 X. Lang, A. Hirata, T. Fujita, M. Chen, *Nat. Nanotechnol.* **2011**, *6*, 232.

10 M. M. M. Ahmed, T. Imae, *J. Magn. Magn. Mater.* **2019**, *491*, 165604.

11 L. Pan, H. Qiu, C. Dou, Y. Li, L. Pu, J. Xu, Y. Shi, *Int. J. Mol. Sci.* **2010**, *11*, 2636.

12 G. Wang, A. Morrin, M. Li, N. Liu, X. Luo, *J. Mater. Chem. B* **2018**, *6*, 4173.

13 A. Ghosh, Y. H. Lee, *ChemSusChem* **2012**, *5*, 480.

14 M. M. M. Ahmed, T. Imae, J. P. Hill, Y. Yamauchi, K. Ariga, L. K. Shrestha, *Colloids Surf., A* **2018**, *538*, 127.

15 M. C. Fite, T. Imae, *Bull. Chem. Soc. Jpn.* **2020**, *93*, 1139.

16 A. Pal, M. P. Sk, A. Chattopadhyay, *ACS Appl. Mater. Interfaces* **2016**, *8*, 5758.

17 X. Zhang, J. Wang, J. Liu, J. Wu, H. Chen, H. Bi, *Carbon* **2017**, *115*, 134.

18 B. Devadas, T. Imae, *ACS Sustainable Chem. Eng.* **2018**, *6*, 127.

19 C. C. Chang, T. Imae, *ACS Sustainable Chem. Eng.* **2018**, *6*, 5162.

20 S. Zhu, G. Xu, *Nanoscale* **2010**, *2*, 2538.

21 A. Izadi-Najafabadi, T. Yamada, D. N. Futaba, M. Yudasaka, H. Takagi, H. Hatori, S. Iijima, K. Hata, *ACS Nano* **2011**, *5*, 811.

22 Z. Zhang, S. Han, C. Wang, J. Li, G. Xu, *Nanomaterials* **2015**, *5*, 1732.

23 Y.-H. Hsu, H.-L. Hsieh, G. Viswanathan, S. H. Voon, C. S. Kue, W. S. Saw, C. H. Yeong, C. A. Azlan, T. Imae, L. V. Kiew, H. B. Lee, L. Y. Chung, *J. Nanopart. Res.* **2017**, *19*, 359.

24 M. J. Krysmann, A. Kelarakis, P. Dallas, E. P. Giannelis, *J. Am. Chem. Soc.* **2012**, *134*, 747.

25 B. Unnikrishnan, C.-W. Wu, I.-W. P. Chen, H.-T. Chang, C.-H. Lin, C.-C. Huang, *ACS Sustainable Chem. Eng.* **2016**, *4*, 3008.

26 W. Liu, C. Li, Y. Ren, X. Sun, W. Pan, Y. Li, J. Wang, W. Wang, *J. Mater. Chem. B* **2016**, *4*, 5772.

27 L. Xu, X. Dun, J. Zou, Y. Li, M. Jia, L. Cui, J. Gao, X. Jin, *J. Electrochem. Soc.* **2018**, *165*, A2217.

28 M. T. Efa, T. Imae, *Electrochim. Acta* **2019**, *303*, 204.

29 H. F. Etefa, T. Imae, M. Yanagida, *ACS Appl. Mater. Interfaces* **2020**, *12*, 18596.

30 V. C. Hoang, L. H. Nguyen, V. G. Gomes, *J. Electroanal. Chem.* **2019**, *832*, 87.

31 A. Yu, V. Chabot, J. Zhang, CRC Press, **2013**. doi:10.1201/b14671.

32 A. Prasannan, T. Imae, *Ind. Eng. Chem. Res.* **2013**, *52*, 15673.

33 X. Huang, Q. Wang, X. Y. Chen, Z. J. Zhang, *J. Electroanal. Chem.* **2015**, *748*, 23.

34 K. P. Annamalai, J. Gao, L. Liu, J. Mei, W. Lau, Y. Tao, *J. Mater. Chem. A* **2015**, *3*, 11740.

35 B. Fresco-Cala, Á. I. López-Lorente, S. Cárdenas, *Nanomaterials* **2018**, *8*, 370.

36 X. Jian, H.-m. Yang, J.-g. Li, E.-h. Zhang, Z.-h. Liang, *Electrochim. Acta* **2017**, *228*, 483.

37 M. T. Efa, T. Imae, *J. Taiwan Inst. Chem. Eng.* **2018**, *92*, 112.

38 K. Murata, K. Kaneko, H. Kanoh, D. Kasuya, K. Takahashi, F. Kokai, M. Yudasaka, S. Iijima, *J. Phys. Chem. B* **2002**, *106*, 11132.

39 B. Devadas, C. C. Chang, T. Imae, *J. Taiwan Inst. Chem. Eng.* **2019**, *102*, 378.

40 Y.-m. Cai, Z.-y. Qin, L. Chen, *Prog. Nat. Sci.: Mater. Int.* **2011**, *21*, 460.

41 M. Lu, F. Beguin, E. Frackowiak, Supercapacitors: materials, systems and applications, John Wiley & Sons, **2013**.

42 T. A. Geleta, T. Imae, *Bull. Chem. Soc. Jpn.* **2020**, *93*, 611.

43 S. Im, Y. R. Park, S. Park, H. J. Kim, J. H. Doh, K. Kwon, W. G. Hong, B. Kim, W. S. Yang, T. Kim, *Appl. Surf. Sci.* **2017**, *412*, 160.

44 S. Maiti, B. Khatua, *Express Polym. Lett.* **2014**, *8*, 895.

45 D. Wei, H. Wang, P. Hiralal, P. Andrew, T. Ryhänen, Y. Hayashi, G. A J Amaratunga, *Nanotechnology* **2010**, *21*, 435702.

46 A. Afzal, F. A. Abuilaiwi, A. Habib, M. Awais, S. B. Waje, M. A. Atieh, *Power Sources* **2017**, *352*, 174.

47 X. Jian, J.-g. Li, H.-m. Yang, L.-l. Cao, E.-h. Zhang, Z.-h. Liang, *Carbon* **2017**, *114*, 533.

48 C. Bora, J. Sharma, S. Dolui, *J. Phys. Chem. C* **2014**, *118*, 29688.

49 B. S. Singu, P. Srinivasan, K. R. Yoon, *J. Solid State Electrochem.* **2016**, *20*, 3447.